Superparamagnetism in MgO-based magnetic tunnel junctions with a thin pinned ferromagnetic electrode

J. F. Feng,[1,2] J. Y. Chen,[1,2] M. Venkatesan,[1] G. Feng,[1] X. F. Han,[2] and J. M. D. Coey[1]
[1]*School of Physics and CRANN, Trinity College, Dublin, Ireland*
[2]*Beijing National Laboratory for Condensed Matter Physics, Institute of Physics, Chinese Academy of Sciences, 100190 Beijing, China*
(Received 10 December 2009; revised manuscript received 2 April 2010; published 25 May 2010)

MgO-based magnetic tunnel junctions have been fabricated with a thin $Co_{40}Fe_{40}B_{20}$ (CoFeB) layer in the pinned synthetic antiferromagnetic CoFe/Ru/CoFeB stack. An inverted tunneling magnetoresistance is observed due to the unbalanced synthetic antiferromagnet. Superparamagnetic nanoparticles form when the CoFeB layer is thinner than 1.5 nm, and an abnormal temperature dependence of the junction resistance is associated with superparamagnetism when the thermal fluctuation energy exceeds the magnetic anisotropy energy. This explanation accounts for the temperature dependence of the tunneling magnetoresistance effect.

DOI: 10.1103/PhysRevB.81.205212 PACS number(s): 75.70.Ak, 73.40.Rw, 73.40.Gk

I. INTRODUCTION

Ever since the development of useful tunneling magnetoresistance (TMR) at room temperature in magnetic tunnel junctions (MTJs) a decade ago, there has been intense research on spin-polarized tunneling in devices with an amorphous AlO_x barrier[1–4] or a crystalline MgO barrier.[5–11] The basic MTJ structure is a sandwich with two ferromagnetic electrodes separated by a thin insulating barrier, which has applications in magnetic random access memory, read heads, and logic devices. In 2001, Butler *et al.*[5] and Mathon and Umerski[6] predicted the large TMR effect in MTJs with single-crystal MgO barriers; very large TMR ratios of about 200% were subsequently reported in devices with (001)-oriented MgO.[7–9] Furthermore, well-oriented (001) MgO-based MTJs with an unpinned pseudospin valve stack give a TMR ratio of more than 1100% at low temperature and 600% at room temperature.[10] Pinned double barrier MTJs have been reported to show a record TMR ratio of 1056% at room temperature.[11] The positive TMR effect here is defined as $(R_{AP}-R_P)/R_P$, where R_P and R_{AP} are the resistances of the junctions when the moments of the ferromagnetic electrodes in contact with tunnel barrier are parallel and antiparallel, respectively. The high TMR in MgO-based MTJs devices is due to the filtering effect of the crystalline MgO barrier, which depends on symmetry of the $\uparrow$ and $\downarrow$ electron wave functions. The barrier is relatively transparent for the majority-spin electrons injected from an oriented bcc Fe or Fe-Co electrode but it strongly attenuates the minority-spin electrons.[5,6]

In Jullière's simple model of tunneling,[12] TMR is determined by the spin polarization of the total electronic density of states of the ferromagnetic electrodes near the Fermi surface. Many features of the TMR which relate to elastic tunneling have been explained in terms of the spin-polarized electronic band structure of the electrodes.[3,4,7,8] However, TMR is usually suppressed when inelastic tunneling occurs.[13] The inelastic tunneling process may be associated with imperfections, impurities, or clusters that can form in the barrier and at the ferromagnet/barrier interfaces.[13,14] Those above-mentioned factors do not depend on the ferromagnetic nature of the electrodes. From this point of view, the key to enhance the TMR is to improve the quality of both the barrier and the interfaces.

In our previous work, we reported an inverted TMR effect in MTJs when a thin pinned bottom ferromagnetic electrode was used in the pinned synthetic antiferromagnetic (SAF) stack.[15] The inverted TMR was due to the imbalance of the SAF stack. Here we examine the temperature dependence of the junction resistance and the inverted TMR effect for these MgO-based MTJs, which is related to the superparamagnetism. The abnormal temperature dependence of the low junction resistance (R_P) occurs despite the high resistance-area products, which cannot be explained by magnetic impurities or magnon assisted tunneling.[13] We conclude that superparamagnetic nanoparticles in the pinned $Co_{40}Fe_{40}B_{20}$ (CoFeB) layer probably can explain our results.

II. EXPERIMENTAL METHOD

A sequential sputtering method was used for sample preparation.[15] The typical MgO-based MTJ multilayer is Ta(5)/Ru(50)/Ta(5)/$Ni_{81}Fe_{19}$(5)/$Ir_{22}Mn_{78}$(10)/$Co_{90}Fe_{10}$(2) / Ru(0.85) / $Co_{40}Fe_{40}B_{20}(t)$/MgO(2.5) /$Co_{40}Fe_{40}B_{20}$(3)/Ta(5)/Ru(5) (thickness in nanometers) and the order is from the bottom electrode to the top. All multilayers were grown under high vacuum (10^{-7} Torr) and at room temperature in a Shamrock sputtering tool. The thickness (t) of the pinned CoFeB layer was 0.5, 0.75, or 1.0 nm. (001)-oriented MgO barrier can be achieved and a high TMR ratio of 155% was observed in MTJs with a thick pinned CoFeB layer.[15,16] The resistance-area products are of order 10^6 Ω μm^2 and a nonlinear current-voltage characteristic is observed for MgO-based MTJs with a thin CoFeB layer.[15] After depositing the MTJ stack, microscale MTJs were fabricated using conventional UV lithography. High vacuum thermal annealing of the patterned junctions with an area from 12×12 to 24×24 μm^2 was carried out for 1 h in an applied magnetic field of 800 mT. All magnetotransport measurements were performed by a four-probe method. The temperature dependence of the MTJ magnetization of unpatterned samples with a size of 5×5 mm^2, for both zero-field-cooled (ZFC) and field-cooled (FC) data, was measured with a Quantum Design magnetometer.

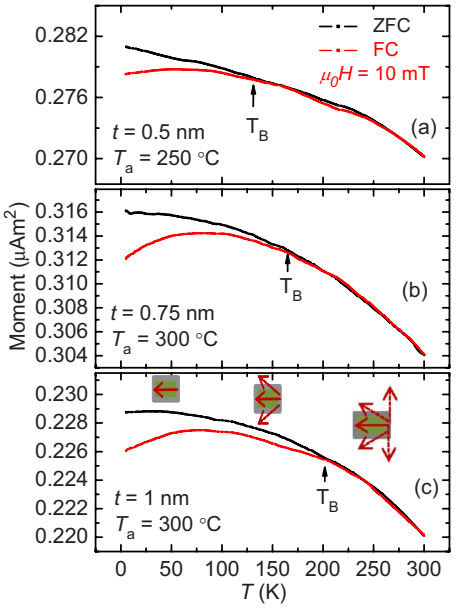

FIG. 1. (Color online) Temperature dependence of the magnetization (M-T) for unpatterned MTJ samples with (a) t=0.5 nm, (b) 0.75 nm, and (c) 1.0 nm, measured with ZFC and FC modes.

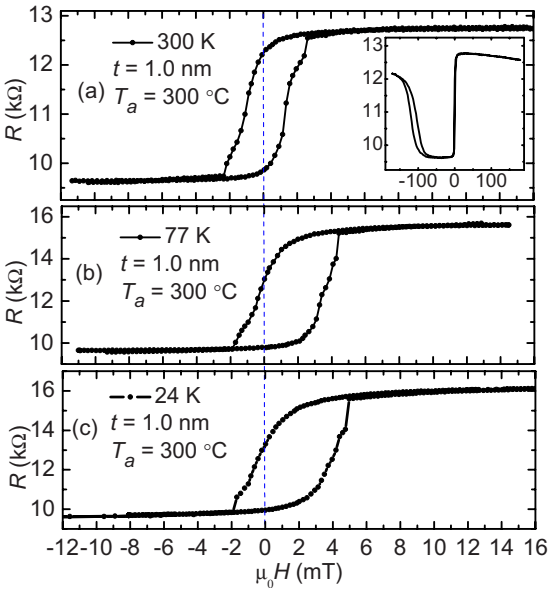

FIG. 2. (Color online) [(a)–(c)] The junction resistance (R) as a function of field at 300 K, 77 K, and 24 K, respectively. Inset in (a) shows the R-$\mu_0 H$ curve over a large field range at 300 K. The pinned CoFeB thickness is 1.0 nm for this MTJ, annealed at 300 °C. The dashed line is of $\mu_0 H$=0.

III. RESULTS AND DISCUSSION

Figures 1(a)–1(c) show the ZFC and FC magnetization curves for unpatterned MTJ samples with t=0.5, 0.75, and 1.0 nm, annealed at a temperature (T_a) of 250 or 300 °C. A magnetic field of 10 mT is applied for the FC curve, which is the same field to set two resistance states of the MTJs. Despite the thick free CoFeB and CoFe layers in MTJ samples, the FC and ZFC curves diverge significantly below a temperature for three samples, for example, around 200 K for the MTJ sample with t=1.0 nm as show in Fig. 1(c). This behavior is not expected for a ferromagnet and suggests the presence of magnetic nanoparticles in the films due to the thin pinned CoFeB layer.[17] The effect is not due to the temperature dependence of the coercivity, which is much less than the applied field. It is very similar to the results observed in MTJs with a thin free CoFeB layer, which shows that superparamagnetic nanoparticles can form in the thin ferromagnetic layer.[18] The nanoparticles develop significant coercivity at low temperature when the magnetic anisotropy energy exceeds the thermal fluctuation energy.[17,18] However, the nonzero TMR effect at room temperature shows there exists a weak magnetization which may come from large-sized particles in the thin pinned CoFeB layer due to a broad size distribution (see below). Here, we focus on the influence of superparamagnetism on the magnetotransport behavior for MTJ devices with a thin pinned CoFeB layer.

Figures 2(a)–2(c) show the free layer switching near zero magnetic field at 300 K, 77 K, and 24 K, respectively. The data are recorded under a small bias voltage of 2 mV. Interestingly, the center of the free CoFeB loop shifts about 1.0 mT in the R-$\mu_0 H$ curves at low temperature compared to that at 300 K. The shift occurs at low temperature, which suggests that extra magnetic coupling occurs as the superparamagnetic CoFeB nanoparticles become blocked. Similar low-temperature shifts are observed for MTJs with t=0.5 and 0.75 nm. The inset of Fig. 1(a) gives the R vs $\mu_0 H$ curve over a large magnetic field range, showing the exchange bias. The TMR effect is inverted in these devices.[15] Here we define

$$\mathrm{TMR} = (R_{low} - R_{high})/R_{low}, \tag{1}$$

where the low (R_{low}) and high (R_{high}) resistance states are defined as the parallel and antiparallel alignments between the pinned and free CoFeB layers on either side of the barrier. Inverted TMR ratios of −33% and −77% are obtained at 300 and 24 K for MTJs with t=1.0 nm, which is less than the positive TMR value of up to 200% found for MTJs with a thicker pinned ferromagnetic layer.[7–11,15,16] The spin filter effect of the crystalline MgO barrier is much suppressed for these MTJs and the suppression should somehow be related to the thickness of the pinned CoFeB layer (see below). Degradation of the MgO layer may also contribute to the lowering of the TMR if the pinned CoFeB layer is not perfectly continuous.

The temperature dependence of the MTJ resistance of Fig. 2 is plotted in Fig. 3(a). The magnetic fields of +10 and −10 mT are separately applied to set the R_{high} and R_{low} states. At 300 K, the R_{high} and R_{low} values are 12.8 kΩ and 9.6 kΩ, respectively. It is clear that R_{high} increases with decreasing temperature. However, the temperature dependence for R_{low} is abnormal. Around 200 K, the R_{low} value begins to decrease as the temperature is lowered. For example, R_{low} is 9.63 kΩ at 200 K and 9.29 kΩ and 24 K. It is found that the abnormal temperature dependence in the R_{low} state is strong for MTJs with the 1.0 nm pinned CoFeB while such behavior in R_{low} is weak for MTJs with t=0.5 and 0.75 nm.[18]

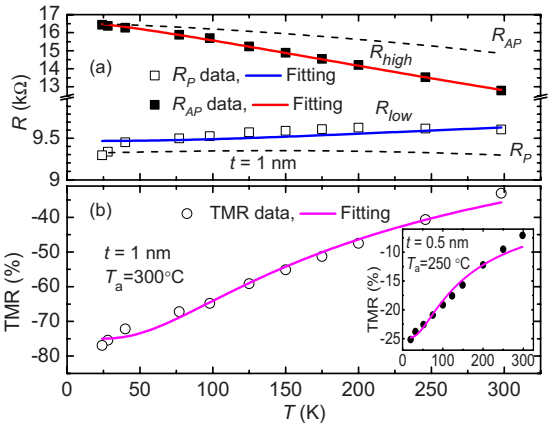

FIG. 3. (Color online) (a) The temperature dependence of R_{low} and R_{high} for one MTJ with t=1.0 nm. The schematic temperature dependence of R_P and R_{AP} for MTJs without nanoparticles is also shown. (b) The temperature dependence of the inverted TMR for the same MTJ as shown in (a). Inset in (b) is the temperature dependence of the inverted TMR for one MTJ with t=0.5 nm. The solid lines (a) and (b) are the fitting results.

The inverted TMR effect appears only when the pinned CoFeB layer in the SAF stack is thin ($t \leq 1.5$ nm).[15] Elastic tunneling is reduced due to the thickness of the pinned CoFeB layer. Furthermore, poorly pinned nanoparticles may appear at the CoFeB/MgO interface if the layer is degraded, which gives rise to an inelastic tunneling. For an MTJ, the temperature dependence of the junction resistance is usually explained in terms of elastic and inelastic tunneling.[14,19] In this picture, the temperature dependence of the averaged conductance in the antiparallel and parallel states of MTJs is given by the following equations:[19]

$$G_P = G_T[1 + P_1P_2] + sT^{1.33},$$

$$G_{AP} = G_T[1 - P_1P_2] + sT^{1.33}, \quad (2)$$

where $G_T = G_0CT/\sin(CT)$, G_0 is the conductance of the MTJ at zero temperature; $C = 1.39 \times 10^{-5} t/(\phi^{1/2})$, with the barrier thickness (t) in nanometers and the barrier height (ϕ) in volts; P_1 and P_2 are effective spin polarizations of two ferromagnetic electrodes and s is a constant. In Eq. (2), the first part represents the elastic tunneling conductance and the second is the inelastic part that follows a power law.[14] The spin polarization at temperature T can be written as[19]

$$P(T) = P_0(1 - \alpha T^{3/2}), \quad (3)$$

where P_0 is the polarization of the electrode at zero temperature and α is a constant associated with spin-wave excitations. By fitting the R_{high} data in Fig. 3(a) using Eqs. (2) and (3), as marked by the red solid line, a good fit is obtained. The same fitting procedure is followed for the R_{low} state, as plotted by a blue solid line. The fitting values of P_0 and α are 56% and 4×10^{-5}, which agrees well with the fitting results in Ref. 19. The inelastic tunneling appears in these MgO-based MTJ devices due to the CoFeB particles at the bottom CoFeB/MgO interface. However, some deviation from the fit occurs for R_{low} and the superparamagnetism may be responsible for it. A sketch of the MTJ structure including superparamagnetic nanoparticles is shown in Fig. 4(a). Spin-flip scattering can occur due to the thermal fluctuation of superparamagnetic nanoparticles in the high-temperature range, which increases the R_{low} value and decreases the R_{high} value.[20] For normal MTJs with thick pinned CoFeB and without any nanoparticles, the schematic temperature dependence of R_{AP} and R_P is shown in Fig. 2(a) and a higher TMR at room temperature can be obtained. Figure 5 shows the temperature dependence of TMR when the superparamagnetism is partly suppressed by an applied magnetic field. Here two states of TMR are defined at 10 and 0 mT for a strong superparamagnetism while they are defined at 10 and −35 mT (much larger than the coercivity of nanoparticles[18]) for the "weak superparamagnetism." This larger field can effectively reduce the superparamagnetism of particles.[17] The TMR curve with the strong superparamagnetism fitted to Eq. (4) below and the fit is very good. In fact, a greater TMR is observed at high temperature when the superparamagnetism is weak.

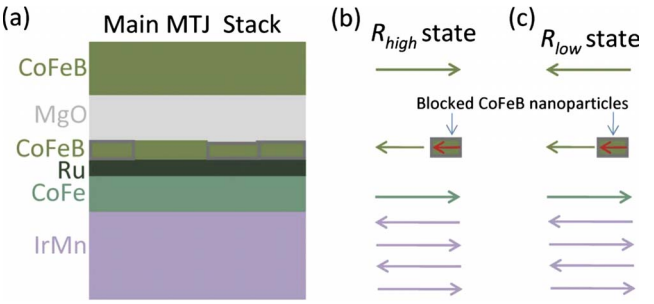

FIG. 4. (Color online) (a) Main structure of MgO-based MTJs including the nanoparticles. (b) and (c) The magnetic switching of the MgO-based MTJs with the CoFeB nanoparticles at antiparallel and parallel states.

The TMR difference (ΔTMR) between two cases shown in the inset of Fig. 5 suggests that the spin-flip scattering reduces the TMR. The ΔTMR value decrease around room

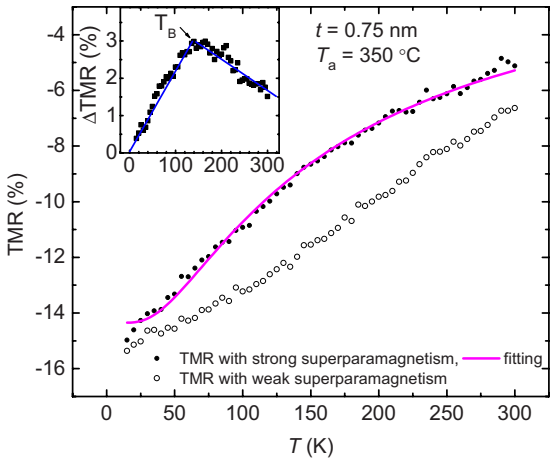

FIG. 5. (Color online) The temperature dependence of TMR with strong and weak superparamagnetism for one MTJ with t =0.75 nm at T_a=350 °C. Inset shows the TMR difference (ΔTMR) between the strong and weak superparamagnetism.

temperature is due to the inelastic tunneling coming from the nanoparticles, which can suppress TMR.[13] Then the ΔTMR increases with lowing temperature until the superparamagnetic particles become blocked, reflecting the decrease in thermal fluctuations of these particles and a broad distribution of particle size. After that, the gradual change in the ΔTMR in the low-temperature range suggests that the enhanced magnetic properties of nanoparticles and lack of spin-flip scattering, which may be responsible for the gradual decease in the low junction resistance with the decrease in temperature. The ΔTMR curve with temperature indicates how the spin-flip scattering influences the transport mechanism of these MTJs. A schematic magnetic switching of these MgO-based MTJs is given in Figs. 4(b) and 4(c), which includes the CoFeB nanoparticles when they are magnetically blocked. Except for the superparamagnetic nanoparticles, the pinned CoFeB layer shows a small moment at room temperature that can be shown by the imbalance of the SAF stack and the nonzero TMR effect at room temperature.[15] Both factors can reduce the spin filter effect of the crystalline MgO barrier, which is the main reason for a relatively low TMR observed for MgO-based MTJs with a thin pinned CoFeB layer.

For normal MTJs with thick ferromagnetic electrodes, the tunneling spin polarization has a temperature dependence as shown in Eq. (3).[19] However, because the pinned CoFeB layer has a small moment for these MgO-based MTJs, the elastic tunneling from this layer is weak, which may have a small influence on the TMR-T curve. It is found that the TMR ratio at 24 K is 2.3 times higher than that at 300 K for MgO-based MTJs with $t=1.0$ nm (see Fig. 3). Here, we focus on the influence of the superparamagnetism on the TMR effect with temperature. Because the superparamagnetic nanoparticles show a thermally activated spin-flip scattering, the TMR effect with temperature for these MTJs may follow a relation,[21]

$$\mathrm{TMR} \propto 1 - \exp(-\Delta/k_B T), \tag{4}$$

where Δ is the activation energy of the superparamagnetic nanoparticles and k_B is the Boltzmann constant. If we use Eq. (4) to fit the TMR data as shown in Fig. 3(b), the average activation energies for MTJs with $t=1.0$ and 0.5 nm are 16.3 ± 0.5 and 11.4 ± 0.7 meV, which correspond to temperatures of 193 ± 6 K and 135 ± 9 K, respectively. In fact, a broad superparamagnetic transition appears around 200 and 130 K for $t=1.0$ and 0.5 nm, according to the M-T curves in Fig. 1, which suggests that Eq. (4) is a good choice to describe the temperature dependence of the TMR effect for MTJs with superparamagnetic nanoparticles that contribute to spin-flip scattering. Moreover, the transition temperature for the MTJs with $t=0.75$ nm, is around 165 K according to Fig. 1 and is seen to be about 140 K when one looks at the ΔTMR-T curve shown in the inset of Fig. 5. Figure 6 shows the effective blocking temperature for different thickness of the pinned CoFeB. It can be noted that the larger-sized superparamagnetic nanoparticles have a higher T_B, and a higher T_B is obtained for MTJs with $t=1.0$ nm. It is found that a little difference of T_B obtained from the M-T curves

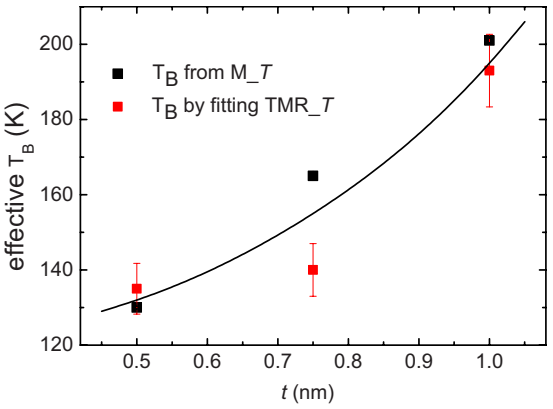

FIG. 6. (Color online) The effective T_B as a function of the thickness (t) of the pinned layer, obtained from the M-T curves and the fitted results. The line is guided to eye.

and the fitted results at each t, which is due to the sample size effect.

It is the superparamagnetic particles that influence the junction resistance and TMR for these MgO-based MTJs. The large change in the TMR ratio with temperature is mainly due to the superparamagnetism. To further understand the effect, we estimate the average size of the CoFeB nanoparticles from the fitted T_B using the following relation:[22]

$$\Delta = 25 k_B T_B. \tag{5}$$

One contribution to the Δ is $K_a V$, where K_a is the magnetic anisotropy constant and V is the volume of a nanoparticle. It is obvious that the CoFeB nanoparticles are metallic. The K_a values for bulk bcc iron and cobalt are 46 $\mathrm{kJ/m^3}$ (Refs. 22 and 23) and 45 $\mathrm{kJ/m^3}$ (Ref. 17), respectively. Another contribution comes from the interface anisotropy (K_i) at the Ru/CoFeB and CoFeB/MgO interfaces. In addition, there is a contribution from shape anisotropy (K_s) which is $\mu_0 M_s(1-3N)/4$,[22] where μ_0 is the permeability of free space, M_s is the saturated magnetization, and N is the demagnetizing factor. Equation (5) can be rewritten as[23]

$$\Delta = (K_a + K_s)V + 2K_i A = (K_a t + K_s t + 2K_i)A = 25 k_B T_B, \tag{6}$$

where $A=\pi r^2$ is the area of a particle, where r is the particle radius. The K_i value is expected to be about 10^{-3} $\mathrm{J/m^2}$ at the interfaces.[22] Obviously K_a and K_i do not necessarily favor the same easy direction. Due to the thin thickness of the CoFeB, it is likely that the interface anisotropy makes the main contribution to the energy barrier. The average particle diameters, D, are 5.2 and 4.5 nm for MTJs with $t=1.0$ nm and 0.5 nm, respectively. Comparable sizes are found for the cobalt in $\mathrm{Co/Al_2O_3}$ multilayers prepared by the sputtering method.[24,25] These particles in the pinned CoFeB layer are large to show superparamagnetism.[17] There will be some distribution of particle size and therefore a distribution of Δ. If we suppose the blocked particles in the tail of the distribution gives rise to the room-temperature TMR, then we can estimate the half width of the distribution in particle size is

$2\delta r=1.6$ nm for MTJs with $t=1.0$ nm and $2\delta r=0.6$ nm for MTJs with $t=0.5$ nm, respectively. Based on the above analysis, the small TMR at room temperature in junctions with a thin pinned CoFeB may arise from larger-sized particles in the layer which are blocked but thermal fluctuation of the smaller superparamagnetic particles may also reduce the TMR (see Fig. 1) as well as imperfection in the MgO layer.

IV. CONLUSIONS

Superparamagnetic nanoparticles form when MgO-based MTJs are fabricated with a sputtered CoFeB layer thinner than 1.5 nm in the pinned synthetic antiferromagnetic stack. The larger-sized nanoparticles which have a blocking temperature above room temperature are responsible for the unbalanced SAF stack, which causes the inverted TMR observed at room temperature in these MTJs. The TMR effect increases at low temperature as $1-\exp(-\Delta/k_BT)$ due to the blocking of the smaller particles at low temperatures. Spin-flip scattering occurs due to the thermal fluctuation of nanoparticles, which are above the blocking temperature. Our results illustrate the correlation between the magnetotransport properties and superparamagnetism.

ACKNOWLEDGMENTS

This work was supported by Science Foundation Ireland as part of the MANSE projects and by the EU as part of the BIOMAGSENS project. We are also grateful for the partial support of the State Key Project of Fundamental Research, Ministry of Science and Technology (MOST) under Grant No. 2006CB932200, Chinese National Natural Science Foundation (NSFC) under Grants No. 10574156, No. 50528101, and No. 50721001, and Ireland-China Joint Research Project supported by SFI and MOST.

[1] T. Miyazaki and N. Tezuka, J. Magn. Magn. Mater. **139**, L231 (1995).
[2] J. S. Moodera, L. R. Kinder, T. M. Wong, and R. Meservey, Phys. Rev. Lett. **74**, 3273 (1995).
[3] X. F. Han, M. Oogane, H. Kubota, Y. Ando, and T. Miyazaki, Appl. Phys. Lett. **77**, 283 (2000).
[4] D. Wang, C. Nordman, J. M. Daughton, Z. Qian, and J. Fink, IEEE Trans. Magn. **40**, 2269 (2004).
[5] W. H. Butler, X.-G. Zhang, T. C. Schulthess, and J. M. MacLaren, Phys. Rev. B **63**, 054416 (2001).
[6] J. Mathon and A. Umerski, Phys. Rev. B **63**, 220403 (2001).
[7] S. S. P. Parkin, C. Kaiser, A. Panchula, P. M. Rice, B. Hughes, M. Samant, and S.-H. Yang, Nat. Mater. **3**, 862 (2004).
[8] S. Yuasa, T. Nagahama, A. Fukushima, Y. Suzuki, and K. Ando, Nat. Mater. **3**, 868 (2004).
[9] D. D. Djayaprawira, K. Tsunekawa, M. Nagai, H. Maehara, S. Yamagata, N. Watanabe, S. Yuasa, Y. Suzuki, and K. Ando, Appl. Phys. Lett. **86**, 092502 (2005).
[10] S. Ikeda, J. Hayakawa, Y. Ashizawa, Y. M. Lee, K. Miura, H. Hasegawa, M. Tsunoda, F. Matsukura, and H. Ohno, Appl. Phys. Lett. **93**, 082508 (2008).
[11] L. X. Jiang, H. Naganuma, M. Oogane, and Y. Ando, Appl. Phys. Express **2**, 083002 (2009).
[12] M. Julliere, Phys. Lett. A **54**, 225 (1975).
[13] F. Guinea, Phys. Rev. B **58**, 9212 (1998).
[14] C. H. Shang, J. Nowak, R. Jansen, and J. S. Moodera, Phys. Rev. B **58**, R2917 (1998).
[15] J. F. Feng, G. Feng, J. M. D. Coey, X. F. Han, and W. S. Zhan, Appl. Phys. Lett. **91**, 102505 (2007).
[16] G. Feng, S. van Dijken, and J. M. D. Coey, Appl. Phys. Lett. **89**, 162501 (2006).
[17] S. R. Shinde, S. B. Ogale, J. S. Higgins, H. Zheng, A. J. Millis, V. N. Kulkarni, R. Ramesh, R. L. Greene, and T. Venkatesan, Phys. Rev. Lett. **92**, 166601 (2004).
[18] Y. M. Jang, C. H. Nam, J. Y. Kim, B. K. Cho, Y. J. Cho, and T. W. Kim, Appl. Phys. Lett. **89**, 163119 (2006).
[19] L. Yuan, S. H. Liou, and D. X. Wang, Phys. Rev. B **73**, 134403 (2006).
[20] Z.-G. Zhu, G. Su, Q.-R. Zheng, and B. Jin, Phys. Lett. A **300**, 658 (2002).
[21] C. T. Black, C. B. Murray, R. L. Sandstrom, and S. H. Sun, Science **290**, 1131 (2000).
[22] J. M. D. Coey, *Magnetism and Magnetic Materials* (Cambridge University, Cambridge, England, 2010).
[23] C. Martínez Boubeta, C. Clavero, J. M. García-Martín, G. Armelles, A. Cebollada, Ll. Balcells, J. L. Menéndez, F. Peiró, A. Cornet, and Michael F. Toney, Phys. Rev. B **71**, 014407 (2005).
[24] J. Briático, J.-L. Maurice, J. Carrey, D. Imhoff, F. Petroff, and A. Vaurès, Eur. Phys. J. D **9**, 517 (1999).
[25] F. Luis, J. M. Torres, L. M. García, J. Bartolomé, J. Stankiewicz, F. Petroff, F. Fettar, J.-L. Maurice, and A. Vaurès, Phys. Rev. B **65**, 094409 (2002).